

# Ursolic Acid Inhibits the Activation of Kupffer Cells by Caspase-11/NLRP3 Inflammasome Signaling Pathways

**Yuan Nie**

First Affiliated Hospital of Nanchang University

**Chen-kai Huang**

First Affiliated Hospital of Nanchang University

**Cong Liu**

First Affiliated Hospital of Nanchang University

**Xuan Zhu** (✉ [waiyongtg@163.com](mailto:waiyongtg@163.com))

First Affiliated Hospital of Nanchang University <https://orcid.org/0000-0001-7367-2359>

---

## Research Article

**Keywords:** Kupffer cells, Caspase-11, NLRP3 inflammasome, Ursolic acid, liver fibrosis, hepatic stellate cells

**Posted Date:** February 11th, 2021

**DOI:** <https://doi.org/10.21203/rs.3.rs-166103/v1>

**License:**   This work is licensed under a Creative Commons Attribution 4.0 International License.

[Read Full License](#)

---

# Abstract

**Background:** Previous studies have indicated that Kupffer cells (KCs) are the main regulatory cells for the activation of hepatic stellate cells (HSCs), and caspase-11/NLRP3 inflammasome signaling plays crucial roles in the activation of monocyte-macrophages. Ursolic acid (UA) is a traditional Chinese medicine with antifibrotic effects, but the molecular mechanism underlying these effects is still unclear.

**Methods:** A mouse primary Kupffer cell line in vitro and liver fibrosis mice (including specific gene knockout mice) in vivo were selected as experimental objects. RT-qPCR and Western blotting techniques were utilized to assess the mRNA and protein expression in each group. ELISA and histological analysis were utilized to assess liver injury and collagen deposition.

**Results:** In vitro, caspase-11/NLRP3 inflammasome signaling promoted the activation of Kupffer cells, and UA inhibited the activation of Kupffer cells by caspase-11/NLRP3 inflammasome signaling. In vivo, UA reversed liver damage and fibrosis in fibrotic mice and was related to Kupffer cells; the expression of Caspase-11/NLRP3 inflammasome signaling in Kupffer cells of the UA group was inhibited. Even in the CCl<sub>4</sub> group, the liver damage and fibrosis of NLRP3 knockout mice were alleviated, and related experiments also proved that the inhibitory effect of UA on Kupffer cells was related to the activation of the NLRP3 inflammasome.

**Conclusion:** Caspase-11/NLRP3 inflammasome signal transduction is closely related to the activation of Kupffer cells and the occurrence of liver fibrosis. Additionally, caspase-11/NLRP3 inflammasome signaling serves as a new target for UA antifibrosis treatment.

## Introduction

Liver fibrosis is an over repair response caused by various chronic liver injuries characterized by excessive deposition of extracellular matrix (ECM) and dominated by type I collagen in the liver<sup>[1]</sup>. The continuous development of liver fibrosis can eventually lead to cirrhosis and even liver cancer, which seriously harms human health<sup>[2]</sup>. Activated hepatic stellate cells (HSCs) are the main source of ECM, and the activation and transformation process of hepatic fibrosis is the central event. Overall, inhibition of the activation of HSCs is the key factor controlling the progression of liver fibrosis<sup>[1]</sup>. Kupffer cells (KCs) are the main regulatory cells in the process of liver fibrosis and activate hepatic stellate cells in the resting state to promote liver fibrosis<sup>[3]</sup>. Cytokines secreted by activated Kupffer cells can directly affect the activation of HSCs, including TGF- $\beta$ , IL-1 $\beta$ , INF, and CCL3. Proinflammatory factors promote HSC activation through the NF- $\kappa$ B signaling pathway, such as TNF and IL-1 $\beta$ . CCL3 is a ligand of CCR1 and CCR5, which promote liver fibrosis<sup>[4]</sup>. Kupffer cells can also produce IL-1 receptor antagonist (IL-1Ra), IL-10 and other anti-inflammatory mediators and can produce matrix metalloproteinase (MMP) to promote the degradation of ECM and improve liver fibrosis<sup>[5]</sup>. Kupffer cells (KCs) play a key role in regulating HSC activation and liver fibrosis progression.

The NOD-like receptor protein 3 inflammasome (NLRP3 inflammasome) consists of pattern recognition receptors (PRRs) and apoptosis-associated speck-like protein containing a caspase-recruitment domain (ASC) and caspase-1 and is a classic intracellular innate immune receptor that can be activated by internal and external danger signals to induce the release of IL-1, IL-18 and other proinflammatory cytokines<sup>[6]</sup>. Studies have shown that the NLRP3 inflammasome activation mechanism is divided into two kinds: through the NLRP3/ASC pathway, activated Caspase 1 is often referred to as the classic NLRP3 inflammasome pathway; however, caspase 11 can also be recruited and activated to activate caspase 1 through NLRP3, resulting in the release of IL-1 $\beta$  and IL-18 and inflammatory cell death, which is a nonclassical NLRP3 inflammasome pathway<sup>[7]</sup>. It has been reported that caspase11<sup>-/-</sup> mice have stronger resistance to lethal sepsis, and their survival rate is significantly higher than that of caspase1<sup>-/-</sup> mice and wild-type mice<sup>[7]</sup>. The activation of caspase 11 is more harmful to the body, which indicates that the nonclassical NLRP3 inflammasome pathway plays a more important role in inflammatory injury progression<sup>[8]</sup>. Ursolic acid (UA) is a natural monomer compound extracted from traditional Chinese medicine plants and has anti-inflammatory, anti-fibrosis, and liver protection effects<sup>[9, 10]</sup>. However, whether ursolic acid has an inhibitory effect on Kupffer cell activation and whether the inhibitory effect is related to the nonclassical Caspase-11/NLRP3 inflammasome pathway remain to be further studied. This study mainly explores the potential mechanism of ursolic acid against fibrosis and provides strong experimental support for the future clinical application of ursolic acid in the treatment of patients with liver fibrosis.

## Materials And Methods

### Reagents and Antibodies

The following reagents were used in this study: CCl<sub>4</sub> and olive oil (Shandong Xiya Chemical Industries Co., Ltd., Shandong, China); UA (Sigma Chemical Co., St. Louis, United States). Anti-Caspase-11 (cat #: ab22684), anti-NLRP (cat #: ab263899), anti-Caspase-1 (cat #: ab138483), anti- $\alpha$ -SMA (cat #: ab32575), anti-Collagen-I (cat #: ab6308), and F4/80 antibodies (cat #: ab6640) were purchased from Abcam (Cambridge, MA, United States). The anti-GAPDH antibody was purchased from OriGene (cat #: TA802519) (Rockville, MD, United States) and horseradish peroxidase-labeled goat anti-mouse IgG and goat anti-rabbit IgG antibodies (Beijing Zhongshan Golden Bridge Biotechnology, Co., Ltd., Beijing, China). Mouse enzyme-linked immunosorbent assay (ELISA) kits for alanine aminotransferase (ALT), aspartate aminotransferase (AST), hydroxyproline, interferon- $\gamma$  (IFN- $\gamma$ ), transforming growth factor- $\beta$  (TGF- $\beta$ ), interleukin-1 $\beta$  (IL-1 $\beta$ ), and tumor necrosis factor alpha (TNF- $\alpha$ ) were purchased from Shanghai Tongwei Industry Co., Ltd.

### Experimental model and design

The primary liver Kupffer cell line was purchased from Jennio Biotech Co., Ltd. (Guangzhou, China) and cultured in Dulbecco's modified Eagle's medium (DMEM) (HyClone, South Logan, UT, USA) supplemented with 10% fetal bovine serum (FBS, Gibco, Grand Island, NY, United States) at 37°C and 5% CO<sub>2</sub>. For the experiments, the Kupffer cells of LPS+H<sub>2</sub>O<sub>2</sub> groups were treated with DMEM containing LPS(1 ng/mL) and H<sub>2</sub>O<sub>2</sub> (10 μmol/L); the Kupffer cells of UA groups were pretreated with DMEM containing UA (10 μmol/L) for 30 min and then treated like the LPS+ H<sub>2</sub>O<sub>2</sub> groups; the Kupffer cells of LPS+ H<sub>2</sub>O<sub>2</sub>+MCC (NLRP3 inhibitors) groups were pretreated with DMEM containing MCC950 (10 μmol/L) for 60 min and then treated like the LPS+ H<sub>2</sub>O<sub>2</sub> groups; the Kupffer cells of LPS+H<sub>2</sub>O<sub>2</sub>+ Wedelolactone (Caspase-11 inhibitors) groups were pretreated with DMEM containing Resveratrol (10 μmol/L) for 60 min and then treated like the LPS+ H<sub>2</sub>O<sub>2</sub> groups<sup>[11, 12]</sup>.

The wild-type (WT) C57BL/6 mice used in the experiments were from the Department of Laboratory Animal Science of Nanchang University, and NLRP3 knockout C57BL/6 mice were purchased from the Jackson Laboratory (homozygous: B6.129S6-Nlrp3<sup>tm1Bhk</sup>/J). Based on widely recognized research, carbon tetrachloride (CCl<sub>4</sub>) was selected to induce liver fibrosis in mice<sup>[13]</sup>. According to the principle of random allocation, male C57BL/6 mice weighing 20 to 30 g were randomly divided into the control group [n = 10, gavage with olive oil (2 ml/kg) twice a week for 8 weeks], CCl<sub>4</sub> group [n = 10, gavage with CCl<sub>4</sub> at 2 ml/kg (20% olive oil dilution) twice a week for 8 weeks], and UA group [n = 10, gavage with CCl<sub>4</sub> at 2 ml/kg (20% olive oil dilution) twice a week for 4 weeks and then gavage with CCl<sub>4</sub> and UA (40 mg/kg/day) gavage for 4 weeks]. Male NLRP3 knockout mice were randomly divided into the NLRP3<sup>-/-</sup> group, NLRP3<sup>-/-</sup> +CCl<sub>4</sub> group and NLRP3<sup>-/-</sup>+ UA group (all treatments were consistent with the WT group). If the mice feel painful during modeling or perfusion, it needs to be killed as soon as possible. Mice were euthanized by inhaling isoflurane and then cervical dislocation, and death was confirmed by neck tissue separation. All experimental procedures were approved by the Institutional Animal Care and Use Committee of the First Affiliated Hospital of Nanchang University (Nanchang, China). All animals received humane care in compliance with institutional guidelines.

## Histological analysis

The paraffin-embedded liver and ileum samples were used to prepare 5 μm thick slices with a microtome. The slices were stained with hematoxylin and eosin using standard methods. Sections underwent hematoxylin and eosin (HE) staining, Sirius red collagen staining and immunohistochemistry (IHC) analysis and were evaluated by microscopy. IHC was used to determine the localization and expression of related proteins. Specimens were incubated with an appropriate antibody and were observed and photographed by confocal microscopy. In immunofluorescence cytochemistry, nuclei were counterstained with DAPI. Finally, images were acquired under a fluorescence microscope.

## Western blot analyses

Total protein was obtained from tissue lysates or cell supernatant for Western blotting. The protein levels were determined using a BCA assay kit (Tiangen, Beijing, China). Denatured proteins were separated on 10% Tris-glycine polyacrylamide gels by SDS-PAGE and transferred to PVDF membranes. The membrane was treated with a chemical illuminator, and the protein bands were detected with a luminescent image analyzer (Bio-Rad ChemiDoc MP, USA). The relative level of the target protein is the gray ratio between the target protein strip and the GAPDH band.

## Quantitative real-time RT-PCR (qRT-PCR)

Total RNA was prepared from liver tissue samples or cells using the RNA Simple Total RNA Kit and the Fast Quant RT Kit (Tiangen, Beijing, China). PCR was performed with a reaction mixture containing cDNA template, primers, and TB Green™ Fast qPCR Mix (TaKaRa, Japan) in a Step One Plus Real-Time PCR System (Thermo Fisher Scientific, USA). The relative abundance of the target gene was obtained by comparison with the standard curve. All primers were purchased from Tianyi-Huiyuan Company (Guangzhou, China), and the primer sequences are shown in supplementary Table 1.

## Extraction of primary Kupffer cells

Mice were anesthetized with isoflurane (300-500 ml/min). The abdominal cavity was cut open aseptically, and the inferior vena cava was punctured. The PBS solution was uniformly perfused by the syringe at the same time. The hepatic portal vein was injected with 50 ml of perfusion solution (0.05% collagenase IV) at 37°C and digested for 10 min. In detail, cell sediments were resuspended in 10 ml of RPMI 1640 and centrifuged at 300×g for 5 min at 4°C, the top aqueous phase was discarded, and the cell sediments were reserved. Then, cell sediments were resuspended in 10 ml RPMI 1640 and centrifuged at 50×g for 3 min at 4°C. The top aqueous phase (cleared cell suspension) was transferred into a new 10 ml centrifuge tube and centrifuged at 300×g for 5 min at 4°C, the top aqueous phase was discarded, and the cell sediments were reserved. The cell sediments mainly constrained nonparenchymal cells of the liver, which were KCs, sinusoidal endothelial cells and satellite cells. To purify the obtained cell population further, the method of selective adherence to plastic was used according to Blomhoff et al<sup>[14]</sup>. KCs were identified by immunofluorescence using anti-F4/80 antibody.

## Statistical analysis

Statistical analyses were performed using SPSS software version 22.0 (SPSS Inc., Chicago, IL), and image production was performed using GraphPad Prism 6.0 software. Quantitative data are expressed as the means ± standard deviation (SD), and continuous variables were compared using one-way analysis of variance (ANOVA). If positive, multiple comparisons were carried out using the Nemenyi test. All statistical tests were two-sided, and P <0.05 was considered statistically significant.

## Results

### Ursoic acid (UA) inhibits the activation of Kupffer cells in vitro

As shown in Figure 1A, the expression of CD68 was significantly increased in IHC after LPS combined with H<sub>2</sub>O<sub>2</sub>-stimulated Kupffer cells, revealing that the activation of Kupffer cells was enhanced after stimulation with LPS combined with H<sub>2</sub>O<sub>2</sub>. After Kupffer cells were treated with UA, the CD68 expression of Kupffer cells was significantly decreased compared with that of the LPS +H<sub>2</sub>O<sub>2</sub> groups. To assess the functional activation of Kupffer cells, the INF- $\gamma$ , TGF- $\beta$ , IL-1 $\beta$ , and TNF- $\alpha$  levels in the cell supernatant secreted by Kupffer cells were determined by ELISA and qRT-PCR. As shown in Figure 1B-I, the INF- $\gamma$ , TGF- $\beta$ , IL-1 $\beta$ , and TNF- $\alpha$  levels of the LPS +H<sub>2</sub>O<sub>2</sub> groups were significantly higher than those of the control group; however, the INF- $\gamma$ , TGF- $\beta$ , IL-1 $\beta$ , and TNF- $\alpha$  levels of the UA groups were significantly decreased compared with those of the LPS+H<sub>2</sub>O<sub>2</sub> groups ( $P < 0.05$ ). These results indicate that UA inhibits the activation of Kupffer cells in vitro.

### UA inhibits the activation of Kupffer cells by the Caspase-11/NLRP3 inflammasome pathway in vitro

To confirm the roles of the Caspase-11/NLRP3 inflammasome pathway in the activation of Kupffer cells, Kupffer cells were pretreated with an NLRP3 inflammasome-specific inhibitor (MCC950) or a caspase-11-specific inhibitor (wedelolactone). First, the immunofluorescence, qRT-PCR and Western blot results indicated that NLRP3 inflammasome expression in the LPS+H<sub>2</sub>O<sub>2</sub>+MCC groups was significantly lower than that in the LPS+H<sub>2</sub>O<sub>2</sub> groups ( $P < 0.05$ ). Additionally, the caspase-11 expression of the LPS+H<sub>2</sub>O<sub>2</sub>+Wedelolactone groups was significantly lower than that of the LPS+H<sub>2</sub>O<sub>2</sub> groups ( $P < 0.05$ ). Importantly, the results that the NLRP3 inflammasome expression of LPS +H<sub>2</sub>O<sub>2</sub>+Wedelolactone groups were also lower than LPS+H<sub>2</sub>O<sub>2</sub> groups and LPS+H<sub>2</sub>O<sub>2</sub>+MCC groups had shown that the Caspase-11 is an effective stimulator of NLRP3 inflammasome. Additionally, proinflammatory cytokines (Figure 2I-J) secreted by Kupffer cells were decreased. The results indicated that the expression of the NLRP3 inflammasome or Caspase-11 was significantly inhibited by MCC or wedelolactone, respectively and that the Caspase-11/NLRP3 inflammasome pathway plays a crucial role in the activation of Kupffer cells.

To confirm that UA inhibits the activation of Kupffer cells through the Caspase-11/NLRP3 inflammasome pathway, the relative protein expression of Caspase-11 and the NLRP3 inflammasome pathway (including caspase-11 and NLRP3) in the LPS +H<sub>2</sub>O<sub>2</sub> +MCC group was detected. As shown in Figure 2, the expression of Caspase-11, NLRP3, Caspase-1 in LPS +H<sub>2</sub>O<sub>2</sub> + UA group were similar to LPS+H<sub>2</sub>O<sub>2</sub> + Wedelolactone groups from the results of immunofluorescence, qRT-PCR and Western blot; the expression of Caspase-11, NLRP3 of LPS+H<sub>2</sub>O<sub>2</sub>+UA group were significantly lower than LPS +H<sub>2</sub>O<sub>2</sub> group. The

results indicated that UA inhibits Kupffer cell activation by inhibiting the Caspase-11/NLRP3 inflammasome pathway.

## **UA reverses liver damage and fibrosis in fibrotic mice**

To evaluate the effect of UA on liver fibrosis, liver damage and collagen deposition in mouse livers were measured by HE and Sirius red staining (Figure 3A). The liver lobule structure, collagen deposition and inflammatory cell infiltration of the CCl<sub>4</sub> group were significantly enhanced ( $P<0.05$ ), and the performance of liver fibrosis was significantly improved after UA treatment ( $P<0.05$ ). The ALT, AST, and hydroxyproline levels in mouse serum were determined to evaluate liver function or liver fibrosis (Figure 3B-D). Compared to the control group, the serum levels of ALT, AST and hydroxyproline in the CCl<sub>4</sub> group mice were significantly increased; however, the levels of ALT, AST and hydroxyproline were inhibited in UA-treated fibrotic mice ( $P<0.05$ ). These results indicate that UA can reverse liver damage and fibrosis in vivo.

Type I collagen (collagen-1),  $\alpha$ -SMA, and TIMP-1 often serve as biomarkers of HSC activation, and changes in these biomarkers are often found in the progression of liver fibrosis. At the mRNA levels, the expression levels of type I collagen (collagen-1),  $\alpha$ -SMA, and TIMP-1 in the CCl<sub>4</sub> group were significantly higher than those in the control group, and this increase in type I collagen,  $\alpha$ -SMA, and TIMP-1 was decreased (Figure 3E-G) ( $P<0.05$ ). At the protein level, there was a significant decrease compared with the CCl<sub>4</sub> group (Figure 3H-J) ( $P<0.05$ ).

## **UA reverses liver fibrosis in liver fibrotic mice by the Caspase-11/NLRP3 inflammasome pathway in Kupffer cells**

To confirm the roles of the Caspase-11/NLRP3 inflammasome pathway in liver fibrosis mice and the UA treatment group, immunohistochemical staining of the whole liver tissue of the three groups of mice was conducted. The expression of Caspase-11 and NLRP3 inflammasome of CCl<sub>4</sub> groups were significantly higher than control group, and the expression of Caspase-11 and NLRP3 inflammasome were significantly decreased by UA treatment (Figure 4A).

To further analyze the activation of mouse Kupffer cells in vivo, mouse Kupffer cells were isolated. The results of Kupffer cells isolated by CD14 immunofluorescence showed that the purity of Kupffer cells was good (Supplementary Figure 1E). Caspase-11 was more highly expressed in Kupffer cells than in other liver cells (such as hepatocytes and HSCs) after CCl<sub>4</sub> induction (Supplementary Figure 1A-D). First, the activation of Kupffer cells isolated from the three groups of mice was determined. The results of pro-inflammatory cytokine (INF- $\gamma$ , TGF- $\beta$ ) by ELISA secreted by Kupffer cells in CCl<sub>4</sub> group were significantly higher than control group ( $P<0.05$ ); and the pro-inflammatory cytokine of UA group were obviously decreased than CCl<sub>4</sub> group ( $P<0.05$ ) (Figure 4B-C). To confirm the effect of the Caspase-11/NLRP3

inflammasome pathway on the inhibition of Kupffer cells by UA, the expression of Caspase-11 and the NLRP3 inflammasome in isolated Kupffer cells was detected. Consistent with the vitro results, the expression of Caspase-11, NLRP3 inflammasome in CCl4 group were significantly higher than control group; the expression of Caspase-11, NLRP3 inflammasome in UA group were significantly lower than CCl4 group ( $P < 0.05$ ) (Figure 4D-I).

## Effect of NLRP3 knockout on liver fibrosis and Kupffer activation

To further confirm the role of the Caspase-11/NLRP3 inflammasome pathway in liver fibrosis, male NLRP3 knockout mice were randomly divided into the NLRP3<sup>-/-</sup> group, NLRP3<sup>-/-</sup>+CCl4 group, and NLRP3<sup>-/-</sup>+UA group. As shown in Figure 5A, the liver lobule structure, collagen deposition and inflammatory cell infiltration of the NLRP3<sup>-/-</sup> group, NLRP3<sup>-/-</sup>+CCl4 group, and NLRP3<sup>-/-</sup>+UA group were significantly reversed compared with those of the WT+CCl4 group. Importantly, there was no significant difference between the three groups (NLRP3<sup>-/-</sup> group, NLRP3<sup>-/-</sup>+CCl4 group, NLRP3<sup>-/-</sup>+UA group). The results showed that the levels of ALT, AST, and hydroxyproline in the mouse serum of the three groups were significantly lower than those in the WT+CCl4 groups, and no obvious change was found between the three NLRP3<sup>-/-</sup> groups (Figure 5B-D). The mRNA expression of collagen-1,  $\alpha$ -SMA, and TIMP-1 in the three NLRP3<sup>-/-</sup> groups was significantly lower than that in the WT+CCl4 groups, and the differences among the three NLRP3<sup>-/-</sup> groups were not statistically significant (Figure 5E-G). Kupffer cells were isolated from mice, and the proinflammatory cytokines (INF- $\gamma$  and TGF- $\beta$ ) in Kupffer cells were measured. The mRNA expression of INF- $\gamma$  and TGF- $\beta$  in the three NLRP3<sup>-/-</sup> groups was significantly lower than that in the WT+CCl4 groups, and the expression levels of INF- $\gamma$  and TGF- $\beta$  in the three NLRP3<sup>-/-</sup> groups were similar (Figure 5H-I). Previous results have indicated that the NLRP3 inflammasome plays a key role in liver fibrosis.

To assess the expression change of the Caspase-11/NLRP3 inflammasome, the mRNA and protein expression of Caspase-11 and the NLRP3 inflammasome were detected. As shown in Figure 5J, 5<sup>o</sup>, and 5N, the mRNA and protein expression of the NLRP3 inflammasome were significantly decreased after NLRP3 knockout in mice. Importantly, the Caspase-11 expression of NLRP3<sup>-/-</sup>+CCl4 group after CCl4 induced is still significantly higher than NLRP3<sup>-/-</sup> group, and the Caspase-11 expression of NLRP3<sup>-/-</sup>+CCl4 group after UA treatment were significantly lower than NLRP3<sup>-/-</sup>+CCl4 group. These results suggest that the NLRP3 inflammasome plays an important role in Caspase-11 in liver fibrosis progression ( $P < 0.05$ ) (Figure 5J, 5K, 5M).

## Discussion

Liver fibrosis is a process of extracellular matrix (ECM) deposition or scar formation caused by various factors, including hepatitis viral, nonalcoholic fatty liver, alcoholic fatty liver, biliary or autoimmune liver disease<sup>[1]</sup>. The continuous development of liver fibrosis can eventually develop into liver cirrhosis, even

liver cancer, which seriously endangers human health<sup>[2]</sup>. Liver fibrosis is the early stage of liver cirrhosis. Effective treatment intervention can effectively prevent the progression of the disease<sup>[15]</sup>. Therefore, it is of great significance to develop antifibrosis drugs based on the pathogenesis of liver fibrosis.

The transformation of quiescent HSCs into proliferative myofibroblasts is the central event in the pathogenesis of liver fibrosis; however, Kupffer cells are the main regulatory cells in the process of liver fibrosis<sup>[3]</sup>. The activation of resting HSCs by Kupffer cells can promote the progression of liver fibrosis; the apoptosis or degradation of activated HSCs by Kupffer cells can promote the progression of liver fibrosis. In the progressive stage of liver injury, hepatocyte injury or harmful substances (such as bacteria or lipopolysaccharide (LPS)) can trigger damage-related molecular models (DAMPs) or pathogen-related molecular models (PAMPs) to activate Toll-like receptors (TLRs) or tumor necrosis factor receptors (TNFRs) to stimulate Kupffer cell activation<sup>[16]</sup>. Then, activated Kupffer cells secrete proinflammatory factors, including TGF- $\beta$ , TNF, IL-1 $\beta$  and IFN- $\gamma$ . At the remission stage of liver injury, Kupffer cells transform into inflammatory inhibitors and produce anti-inflammatory mediators, such as IL-1Ra and IL-10<sup>[17, 18]</sup>. Therefore, Kupffer cells play a double-edged sword role in liver fibrosis. Therefore, the activation of Kupffer cells in vivo and in vitro served as the main observation objects in this study. First, this study found that the activation of primary liver Kupffer cells was significantly enhanced after LPS combined with H<sub>2</sub>O<sub>2</sub> stimulation, and the activation could be inhibited by ursolic acid in vitro. The in vitro results indicated that the Caspase-11/NLRP3 nonclassical inflammasome pathway is involved in the activation of Kupffer cells. Next, we demonstrated that UA could reduce CCl<sub>4</sub>-induced liver fibrosis and inhibit Kupffer cell activation after Kupffer cells were isolated from mouse livers. The Caspase-11/NLRP3 inflammasome pathway plays an important role in the activation of Kupffer cells in vivo. Finally, the results of the NLRP3<sup>-/-</sup> mouse experiment showed that the Caspase-11/NLRP3 inflammasome pathway was involved in Kupffer activation.

The NLRP3 inflammasome is an intracellular multiprotein complex that is widely involved in the body's immune response and is related to the pathogenesis of tumors, arteriosclerosis, intestinal inflammation and metabolic diseases<sup>[19]</sup>. The NLRP3 inflammasome consists of PRRs, ASC, and caspase-1 and is widely distributed in monocytes-macrophages, dendritic cells (DCs), lymphocytes, granulocytes and antigen-presenting cells (APCs)<sup>[20]</sup>. The NLRP3 inflammasome is a classical receptor of intracellular innate immunity that can be activated by danger signals inside and outside the cell and then induce the release of downstream proinflammatory factors (IL-1 $\beta$ , IL-18)<sup>[21]</sup>. At present, the NLRP3 inflammasome is expressed in hepatocytes, Kupffer cells, and HSCs in the liver and is activated under certain conditions, eventually leading to the release of IL-1 $\beta$  and IL-18<sup>[22]</sup>. However, the expression level of the NLRP3 inflammasome in Kupffer cells was significantly higher than that in hepatocytes and HSCs, as shown in Supplementary Figure 1. Therefore, previous studies have indicated that Kupffer cells are the main places for the expression, assembly and activation of NLRP3 inflammasome<sup>[23]</sup>. There were two pathways involved in the NLRP3 inflammasome activation mechanism: classic NLRP3 inflammasome pathways (NLRP3/ASC/Caspase-1) and nonclassical NLRP3 inflammasome pathways (Caspase-

11/NLRP3/Caspase-11)<sup>[7]</sup>. Hepatocyte death is induced by activated NLRP3 inflammasomes through the pyrolytic pathway and aggravates the proceeding of NASH<sup>[24]</sup>. Overall, the NLRP3 inflammasome plays a crucial role in the liver inflammation network.

Caspase-11 is an important promoter of the nonclassical pathway of cell pyrolysis. During the progression of liver injury, gram-negative bacteria enter the liver through the portal vein and release lipopolysaccharides (LPS) on the surface to activate Kupffer cells through the TLR pathway<sup>[25]</sup>. LPS enters Kupffer cells in the form of endocytosis and interacts with intracellular caspase-11 to bind and activate it, thus initiating the nonclassical pathway of cell pyrolysis. LPS enters Kupffer cells through endocytosis and interacts with intracellular caspase-11 and activates it, thereby starting the nonclassical pathway of pyrolysis<sup>[26]</sup>. On the one hand, activated caspase-11 can activate the downstream NLRP3 inflammasome, releasing IL-1 $\beta$  and IL-18; on the other hand, the cell-breaking membrane protein GSDMD is activated and destroys the cell membrane, releases the cell content, and causes inflammatory damage<sup>[27]</sup>. The cross-analysis of unbiased RNA sequencing/proteomic analyses identified Caspase-11 (Caspase-4 in humans) as a commonly upregulated gene in alcoholic hepatitis (AH) and patients but not in chronic alcoholic steatohepatitis (ASH) mice and healthy human livers<sup>[28]</sup>. Recent studies have shown that HSPA12A attenuates LPS-induced liver injury by inhibiting caspase-11-mediated hepatocyte pyroptosis via PGC-1 $\alpha$ -dependent acyloxyacyl hydrolase expression<sup>[28]</sup>. Caspase-11 activation is harmful to the body, and its role in the nonclassical NLRP3 inflammasome pathway is critical. In this study,

Our results indicated that uric acid can improve liver fibrosis by inhibiting the Caspase-11/NLRP3 inflammasome pathway of Kupffer cells. In vivo and in vitro, the Caspase-11/NLRP3 inflammasome pathway plays an indispensable role in the activation of Kupffer cells, and uric acid can inhibit the activation of Kupffer cells by the Caspase-11/NLRP3 inflammasome pathway. The results from NLRP3<sup>-/-</sup> mice showed that the NLRP3 inflammasome had an important impact on the activation progression of Kupffer by Caspase-11. There are also some limitations, such as the lack of results regarding the coculture of Kupffer cells and HSCs and the greater number of Caspase-11 intervention results.

In conclusion, our results indicate that the caspase-11/NLRP3 inflammasome pathway plays an important role in the activation of Kupffer cells. Furthermore, UA may reverse liver fibrosis by intervening in the Caspase-11/NLRP3 inflammasome pathway in Kupffer cells. The potential mechanism of UA against liver fibrosis remains unknown. This study aims to clarify the possible molecular targets of UA against liver fibrosis and provide a reasonable experimental basis for the clinical application of UA in the future. Our results provide new insight into the treatment of liver fibrosis with UA; however, further in vivo and in vitro studies are needed to confirm these results.

## **Declarations**

## **Financial support:**

This study was supported by the National Natural Science Foundation of China (grant number: 81960120), “Gan-Po Talent 555” Project of Jiangxi Province (GCZ (2012)-1) and the Postgraduate Innovation Special Foundation of Jiangxi Province (YC2020-B046).

## Acknowledgments:

We would like to thank the National Natural Science Foundation of China for the economic support.

## Credit author statement

YN and CKH contributed equally to this study. YN designed and wrote the manuscript; CKH experimental operation; CL analyzed data. XZ critically revised the manuscript. All of the authors reviewed the manuscript and approved the final version.

Declaration of Competing Interest: The authors declare that there are no conflicts of interest.

## Ethics statement:

The animal study was reviewed and approved by Institutional Animal Care and Use Committee of the First Affiliated Hospital of Nanchang University (Nanchang China).

## Availability of data and materials

The analyzed data sets generated during the study are available from the corresponding author on reasonable request.

## Consent for Publication:

Not applicable.

## References

1. LEE Y A, WALLACE M C, FRIEDMAN, S. L. 2015. Pathobiology of liver fibrosis: a translational success story[J]. *Gut* 64 (5): 830–841.
2. ASRANI S K, DEVARBHAVI, H., and J. EATON, et al. 2019. Burden of liver diseases in the world[J]. *J Hepatol* 70 (1): 151–171.
3. TACKE, F., and H. W. ZIMMERMANN. 2014. Macrophage heterogeneity in liver injury and fibrosis[J]. *J Hepatol* 60 (5): 1090–1096.

4. De, S. E. K. I. E., and MINICIS S GWAK G Y, et al. 2009. CCR1 and CCR5 promote hepatic fibrosis in mice[J]. *J Clin Invest* 119 (7): 1858–1870.
5. FENG, M., J. DING, and M. WANG, et al. 2018. Kupffer-derived matrix metalloproteinase-9 contributes to liver fibrosis resolution[J]. *Int J Biol Sci* 14 (9): 1033–1040.
6. XUE, Y., ENOSI T D, and TAN W H, et al. 2019. Emerging Activators and Regulators of Inflammasomes and Pyroptosis[J]. *Trends Immunol* 40 (11): 1035–1052.
7. CASSON C N, COPENHAVER A M, and ZWACK E E, et al. 2013. Caspase-11 activation in response to bacterial secretion systems that access the host cytosol[J]. *PLoS Pathog* 9 (6): e1003400.
8. HAGAR, J. A., and Y. POWELL D A, AACHOUI, et al. 2013. Cytoplasmic LPS activates caspase-11: implications in TLR4-independent endotoxic shock[J]. *Science* 341 (6151): 1250–1253.
9. IKEDA, Y., A. MURAKAMI, and Y. FUJIMURA, et al. 2007. Aggregated ursolic acid, a natural triterpenoid, induces IL-1beta release from murine peritoneal macrophages: role of CD36[J]. *J Immunol* 178 (8): 4854–4864.
10. CARGNIN S T, GNOATTO, S. B. 2017. Ursolic acid from apple pomace and traditional plants: A valuable triterpenoid with functional properties[J]. *Food Chem* 220: 477–489.
11. DONG, D., and W. ZHONG. 2016. SUN Q, et al. Oxidative products from alcohol metabolism differentially modulate pro-inflammatory cytokine expression in Kupffer cells and hepatocytes[J]. *Cytokine* 85: 109–119.
12. QU, J., Z. YUAN, and G. WANG, et al. 2019. The selective NLRP3 inflammasome inhibitor MCC950 alleviates cholestatic liver injury and fibrosis in mice[J]. *Int Immunopharmacol* 70: 147–155.
13. PEREZ T R. 1983. Is cirrhosis of the liver experimentally produced by CCl4 and adequate model of human cirrhosis?[J]. *Hepatology* 3 (1): 112–120.
14. BLOMHOFF, R., and T. BERG. 1990. Isolation and cultivation of rat liver stellate cells[J]. *Methods Enzymol* 190: 58–71.
15. MARCELLIN, P., E. GANE, and M. BUTI, et al. 2013. Regression of cirrhosis during treatment with tenofovir disoproxil fumarate for chronic hepatitis B: a 5-year open-label follow-up study[J]. *Lancet* 381 (9865): 468–475.
16. FILLIOL, A., PIQUET-PELLORCE C, and RAGUENES-NICOL C, et al. 2017. RIPK1 protects hepatocytes from Kupffer cells-mediated TNF-induced apoptosis in mouse models of PAMP-induced hepatitis[J]. *J Hepatol* 66 (6): 1205–1213.
17. TAN, Q., and J. HU, YU X, et al. The Role of IL-1 Family Members and Kupffer Cells in Liver Regeneration[J]. *Biomed Res Int*, 2016,2016: 6495793.
18. LIU, J., Q. YU, and W. WU, et al. 2018. TLR2 Stimulation Strengthens Intrahepatic Myeloid-Derived Cell-Mediated T Cell Tolerance through Inducing Kupffer Cell Expansion and IL-10 Production[J]. *J Immunol* 200 (7): 2341–2351.
19. RATHINAM V A, FITZGERALD, K. A. 2016. Inflammasome Complexes: Emerging Mechanisms and Effector Functions[J]. *Cell* 165 (4): 792–800.

20. WANG, D., B. DUNCAN, and X. LI, et al. 2020. The role of NLRP3 inflammasome in infection-related, immune-mediated and autoimmune skin diseases[J]. *J Dermatol Sci* 98 (3): 146–151.
21. MRIDHA A R, WREE, A., and A. ROBERTSON, et al. 2017. NLRP3 inflammasome blockade reduces liver inflammation and fibrosis in experimental NASH in mice[J]. *J Hepatol* 66 (5): 1037–1046.
22. WREE, A., A. EGUCHI, and M. D. MCGEOUGH, et al. 2014. NLRP3 inflammasome activation results in hepatocyte pyroptosis, liver inflammation, and fibrosis in mice[J]. *Hepatology* 59 (3): 898–910.
23. BOARU S G, BORKHAM-KAMPHORST E, T. I. H. A. A. L., et al. 2012. Expression analysis of inflammasomes in experimental models of inflammatory and fibrotic liver disease[J]. *J Inflamm (Lond)* 9 (1): 49.
24. MIURA, K., Y. KODAMA, and S. INOKUCHI, et al. 2010. Toll-like receptor 9 promotes steatohepatitis by induction of interleukin-1beta in mice[J]. *Gastroenterology* 139 (1): 323–334.
25. SMITH, C., and X. WANG. 2015. YIN H. Caspases come together over LPS[J]. *Trends Immunol* 36 (2): 59–61.
26. DENG, M., Y. TANG, and W. LI, et al. 2018. The Endotoxin Delivery Protein HMGB1 Mediates Caspase-11-Dependent Lethality in Sepsis[J]. *Immunity* 49 (4): 740–753.
27. ZHAO, Y., and J. SHI. 2018. SHAO F. Inflammatory Caspases: Activation and Cleavage of Gasdermin-D In Vitro and During Pyroptosis[J]. *Methods Mol Biol* 1714: 131–148.
28. KHANOVA, E., R. WU, and W. WANG, et al. 2018. Pyroptosis by caspase11/4-gasdermin-D pathway in alcoholic hepatitis in mice and patients[J]. *Hepatology* 67 (5): 1737–1753.

## Figures

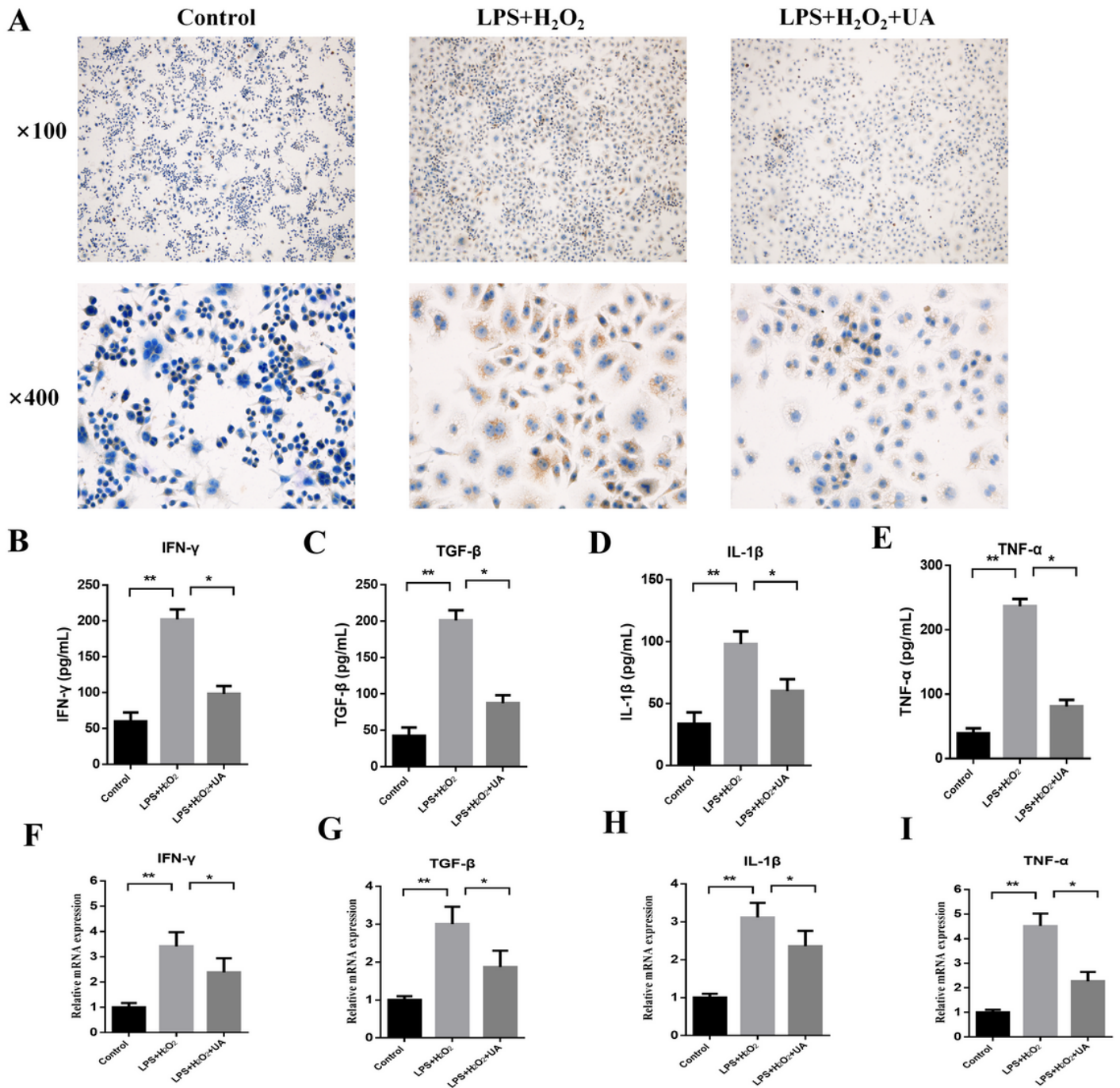


**Figure 1**

The effect of UA on the activation of Kupffer cells by LPS +H<sub>2</sub>O<sub>2</sub>. (A) CD68 immunohistochemistry (100× magnification, 400× magnification) and CD68 (red) staining of Kupffer cells. (B-E) The INF-γ, TGF-β, IL-1β, and TNF-α levels in Kupffer cell supernatant were measured by ELISA. (F-I) mRNA levels of INF-γ, TGF-β, IL-1β, and TNF-α were measured by qRT-PCR. Data represent the mean±SD of each group. \*P<0.05 and \*\*P<0.01.

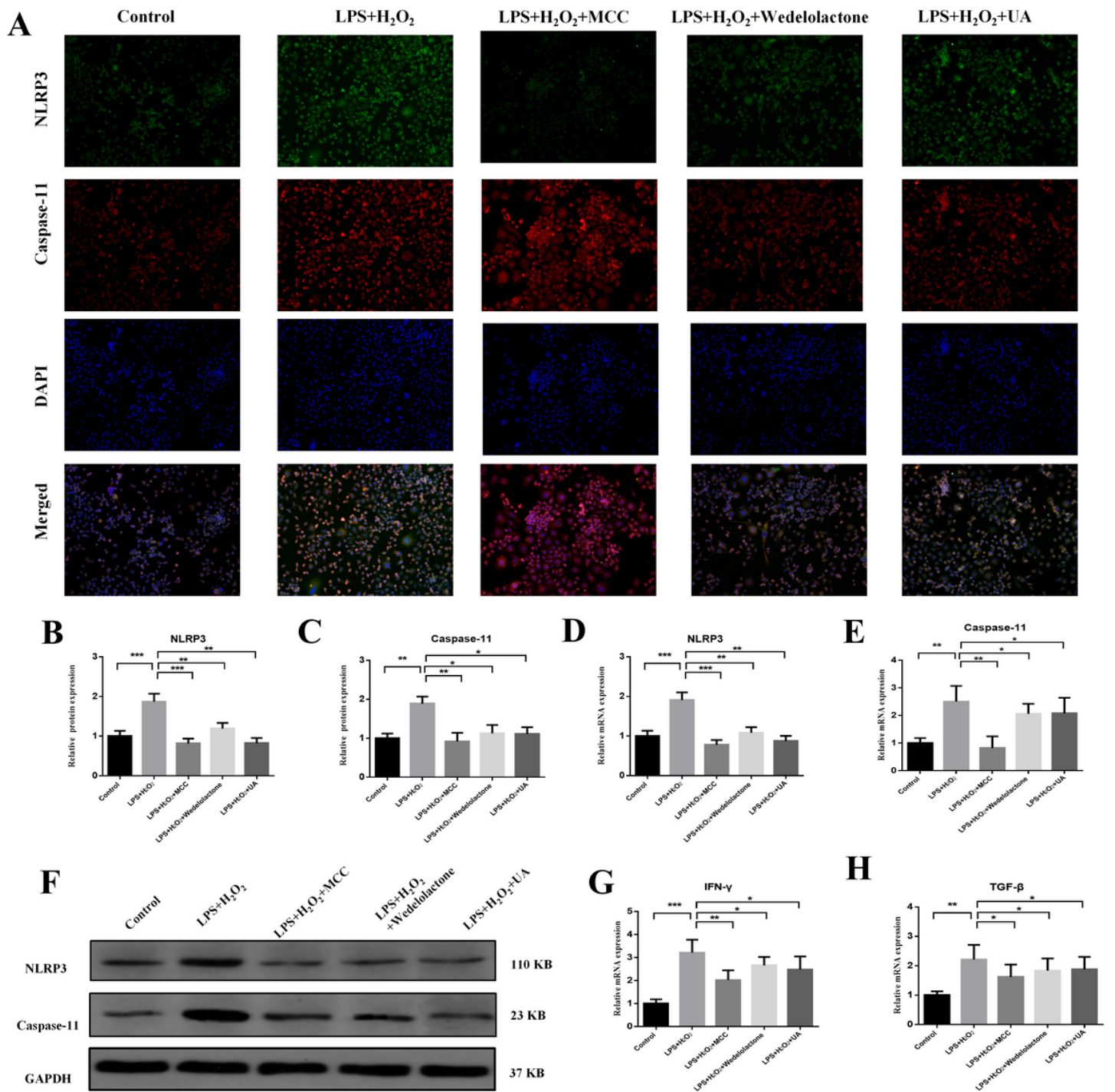


**Figure 2**

The effect of UA on the activation of Kupffer cells by the Caspase-11/NLRP3 inflammasome pathway. (A) Dual immunofluorescence staining of Kupffer cells in control, LPS+H<sub>2</sub>O<sub>2</sub>, LPS+H<sub>2</sub>O<sub>2</sub>+MCC, LPS+H<sub>2</sub>O<sub>2</sub>+ wedelolactone, LPS+H<sub>2</sub>O<sub>2</sub>+UA for nuclei (DAPI, blue), NLRP3 (green), and Caspase-11 (red), and the merged images are shown; (B-C) mRNA levels of Caspase-11 and NLRP3 were measured by qRT-PCR; (D-F) Protein levels of Caspase-11 and NLRP3 were measured by Western blot; (G-H) mRNA levels of IFN-γ and TGF-β were measured by qRT-PCR. Data represent the mean±SD of each group. \*P<0.05 and \*\*P<0.01.

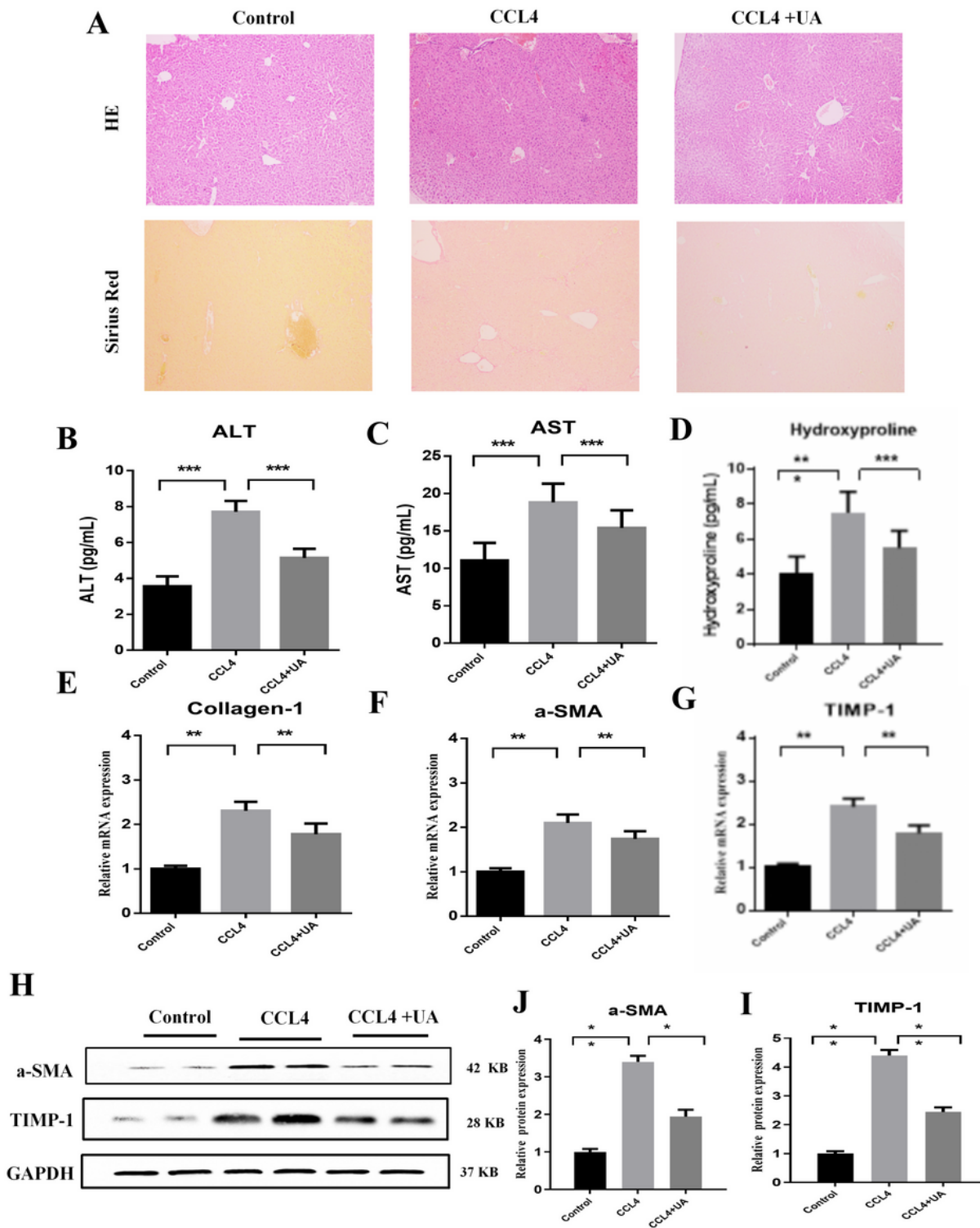


**Figure 3**

The effect of UA on CCl<sub>4</sub>-induced liver injury and fibrosis. (A) HE staining (100× magnification) and Sirius Red (100× magnification) of liver sections from mice in the control, CCl<sub>4</sub> and UA groups; (B-D) The ALT, AST, and hydroxyproline levels in the mouse serum were measured by ELISA; (E-G) mRNA levels of collagen I, α-SMA, and TIMP-1 were measured by qRT-PCR; (H-J) Protein levels of collagen I and α-SMA were measured by Western blot. Data represent the mean±SD of each group. \*P<0.05 and \*\*P<0.01.

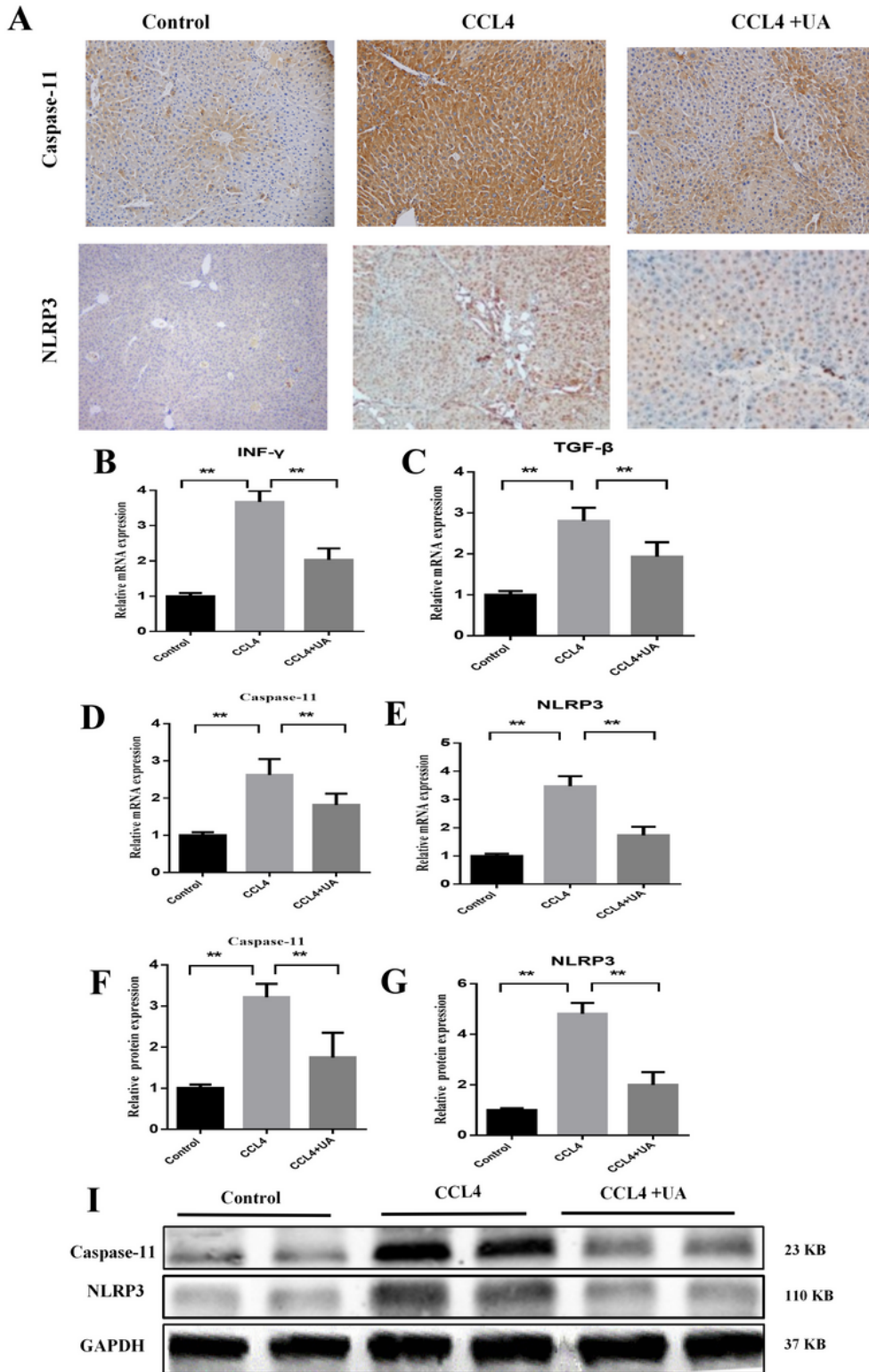


**Figure 4**

The effect of UA on CCL4-induced liver injury and fibrosis by the Caspase-11/NLRP3 inflammasome pathway in Kupffer cells. (A) The expression of Caspase-11 and the NLRP3 inflammasome in whole mouse liver was measured by immunohistochemistry; (B-C) mRNA levels of INF- $\gamma$  and TGF- $\beta$  in isolated Kupffer cells were measured by qRT-PCR; (D-E) mRNA levels of Caspase-11 and NLRP3 in isolated

Kupffer cells were measured by qRT-PCR; (F-I) Protein levels of Caspase-11 and NLRP3 in isolated Kupffer cells were measured by Western blot. Data represent the mean±SD of each group. \*P<0.05 and \*\*P<0.01.

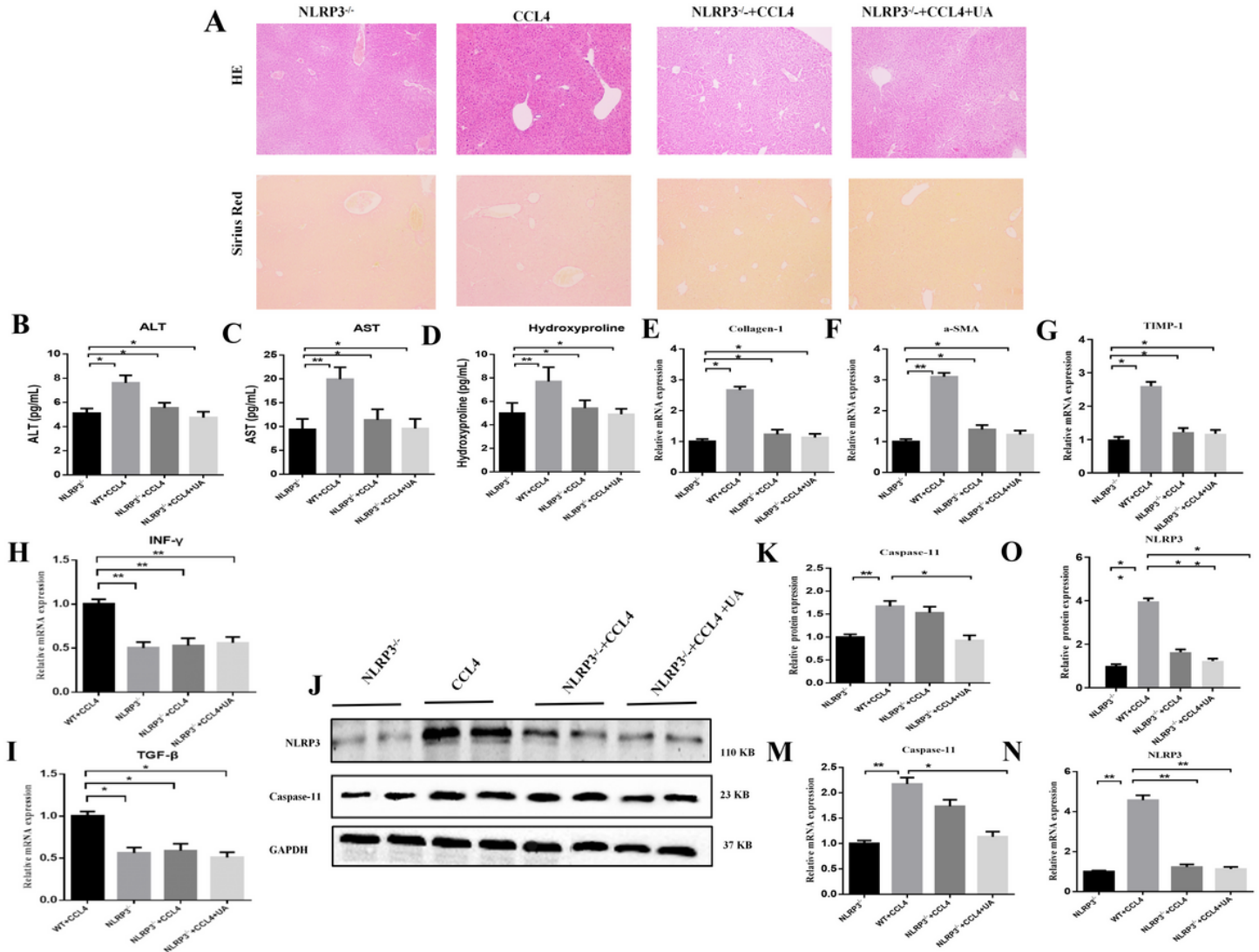


**Figure 5**

Effect of NLRP3 knockout on liver fibrosis and Kupffer activation. (A) HE staining (100× magnification) and Sirius Red (100× magnification) of liver sections from mice in the wild type (WT)+CCI4, NLRP3<sup>-/-</sup>, NLRP3<sup>-/-</sup>+CCI4, NLRP3<sup>-/-</sup>+CCI4+UA; (B-D) The ALT, AST, hydroxyproline level in the mouse serum were measured by ELISA; (E-G) mRNA levels of collagen I, α-SMA, and TIMP-1 were measured by qRT-PCR; (H-I) mRNA levels of INF-γ, TGF-β in isolated Kupffer cells were measured by qRT-PCR; (J-O) Protein levels of Caspase-11, NLRP3 in isolated Kupffer cells were measured by Western blot; (M-N) mRNA levels of Caspase-11, NLRP3 in isolated Kupffer cells were measured by qRT-PCR. Data represent the mean±SD of each group. \*P<0.05 and \*\*P<0.01.

## Supplementary Files

This is a list of supplementary files associated with this preprint. Click to download.

- [SupplementaryFigure1.png](#)
- [Supplementarytable1.docx](#)